Computing energy gaps by Quantum Monte Carlo: applications to high pressure hydrogen

Carlo Pierleoni

Department of Physical and Chemical Sciences
University of L'Aquila, Italy

Collaborators:

David M. Ceperley (UIUC)

Markus Holzmann (CNRS Grenoble)

Vitaly Gorelov (CNRS, Ecole Polytechnique Palaiseau)

Yubo Yang (Paul) (Flatiron Institute)

TREX Bridging Quantum Monte Carlo and High-Performance Simulations, Luxembourg, 5-9 February 2024

Collaborators:

David Ceperley, UIUC USA

Markus Holzmann, CNRS Grenoble

Vitaly Gorelov, CNRS Ecole Polyth, Palaiseau

Yubo Yang, Flatiron

GENCI

NCSA NATIONAL CENTRE FOR SUPERCOMPUTING APPLICATIONS

CINECA

Financial support:

Next-Gen EU

NSF&DOE (USA)

CNRS (France)

Motivations

- **Why computing energy gaps?**
  Energy gaps are important information about the electronic excitations which are often used in experiments to probe the underlying electronic structure of systems.
  Electronic spectra are routinely measured in various spectroscopies, and theoretical methods to compute spectra are available mainly based on DFT and Many Body Perturbation Theory (MBPT).

- **Why computing energy gaps with QMC?**
  QMC is not able to provide electronic spectra directly since this requires computing real time dynamics (dynamical properties).
  Instead QMC is a great method for ground state properties (mainly energy, but also structural properties). Can we extend QMC to compute energy gaps and electronic excitations?
  This will allow to include electronic correlation in the excitation energies in a non-perturbative fashion and provide more accurate values.

Outline

- Energy gaps for static external fields (ideal crystals)
- Finite size effects
- Extension to quantum and thermal crystals
- applications:
  - Carbon and Silicon
  - High Pressure hydrogen

Energy gaps: basic definitions

Charged (single-particle) excitations: *fundamental gap of insulators (quasiparticle)*

$$\Delta_{qp} = E_0(N_e + 1) + E_0(N_e - 1) - 2E_0(N_e)$$

$E_0(N_e)$ = ground state energy of a system with N_e electrons

Neutral (particle-hole) excitation:

$$\Delta_n = E_1(N_e) - E_0(N_e)$$

$E_1(N_e)$ = lowest excited state of a system with N_e electrons

in the first case only GS energies are involved, good for QMC

in the second case an excited state is involved, apparently bad for QMC

Fundamental (quasiparticle) gap

PHYSICAL REVIEW B **101**, 085115 (2020)

Editors' Suggestion

Electronic band gaps from quantum Monte Carlo methods

Yubo Yang (h \ â) ,[1] Vitaly Gorelov,[2] Carlo Pierleoni ,[2,3] David M. Ceperley,[1] and Markus Holzmann[4,5]

$\mu^+ = E_0(N_e + 1) - E_0(N_e)$ chemical potential for adding one electron

$\mu^- = E_0(N_e) - E_0(N_e - 1)$ chemical potential for removing one electron

$\Delta_{qp} = \mu^+ - \mu^- \neq 0$ for gapped systems

In the GrandCanonical ensemble, V and are independent variables while the equilibrium N_e corresponds to the minimum of the Grand Potential

$$\Omega(V,\mu) = \frac{1}{VM_\theta} \sum_\theta \min_{N_e} [E_0(N_e,\theta) - \mu N_e]$$

where indicate that we are using Twisted Boundary Conditions to minimise FSE :

$\Psi(\mathbf{r}_1 + L_x\hat{x}) = e^{i\theta_x}\Psi(\mathbf{r}_1)$

Indicating with $\bar{N}_e(\theta,\mu)$ the optimal number of electron at given (θ,μ), the equilibrium electron and energy densities are respectively

$$n_e(\mu) = (M_\theta V)^{-1} \sum_\theta \bar{N}_e(\theta,\mu) \qquad e_0(\mu) = (M_\theta V)^{-1} \sum_\theta E_0(\bar{N}_e(\theta,\mu),\theta)$$

Hydrogen Ideal crystal C2/c-24 P=248GPa, $N_p = 96$, $N_e = N_p + n$

Total energy (hartrees) vs twist angle (sorted for n=0) for $n \in [-8; +8]$

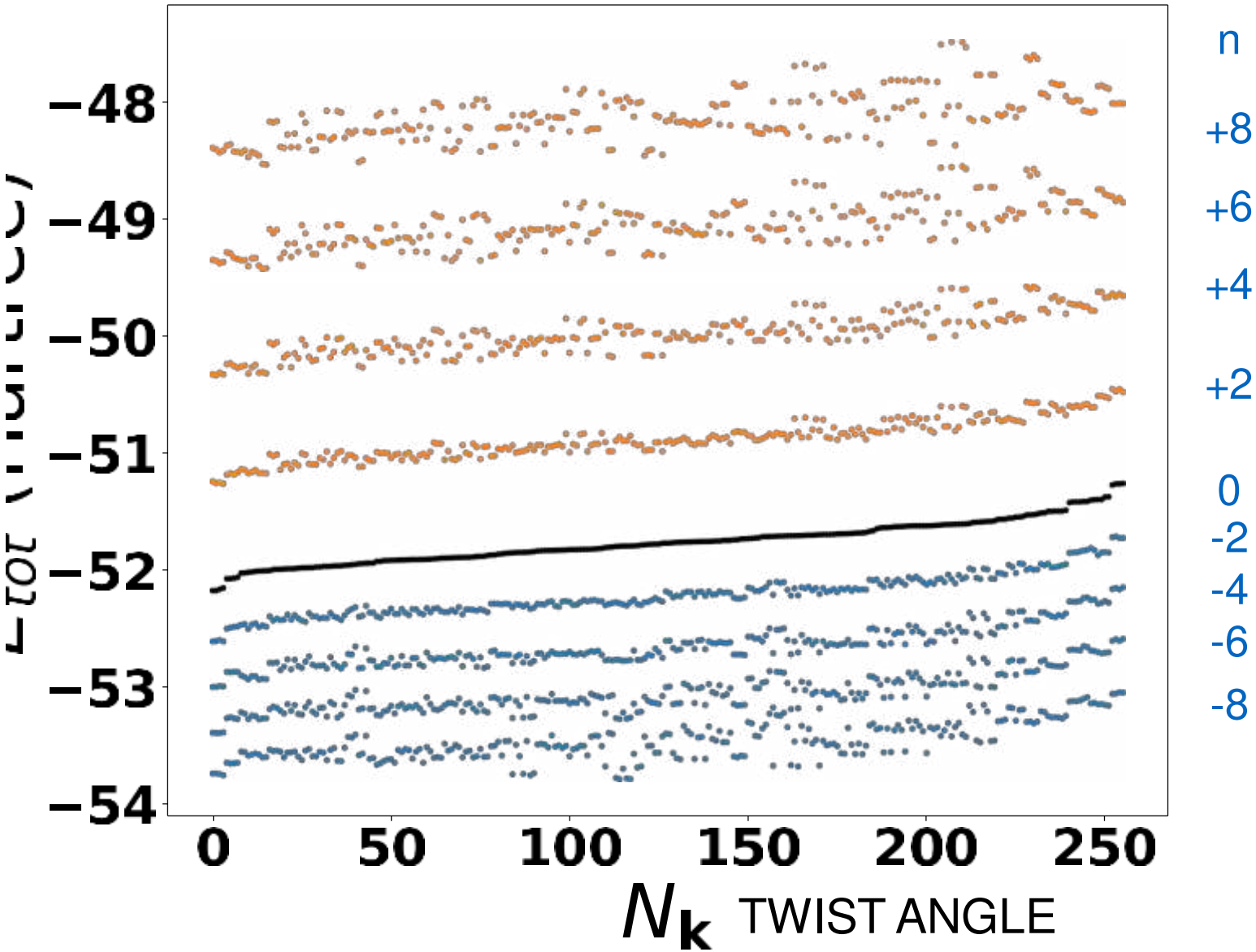

Hydrogen Ideal crystal C2/c-24 P=248GPa, $N_p = 96$, $N_e = N_p + n$

At equilibrium $\frac{\partial E_0}{\partial N_e} = \mu \Longrightarrow E_0(N_e, \theta) - E_0(N_e - 1, \theta) \le \mu \le E_0(N_e + 1, \theta) - E_0(N_e, \theta)$

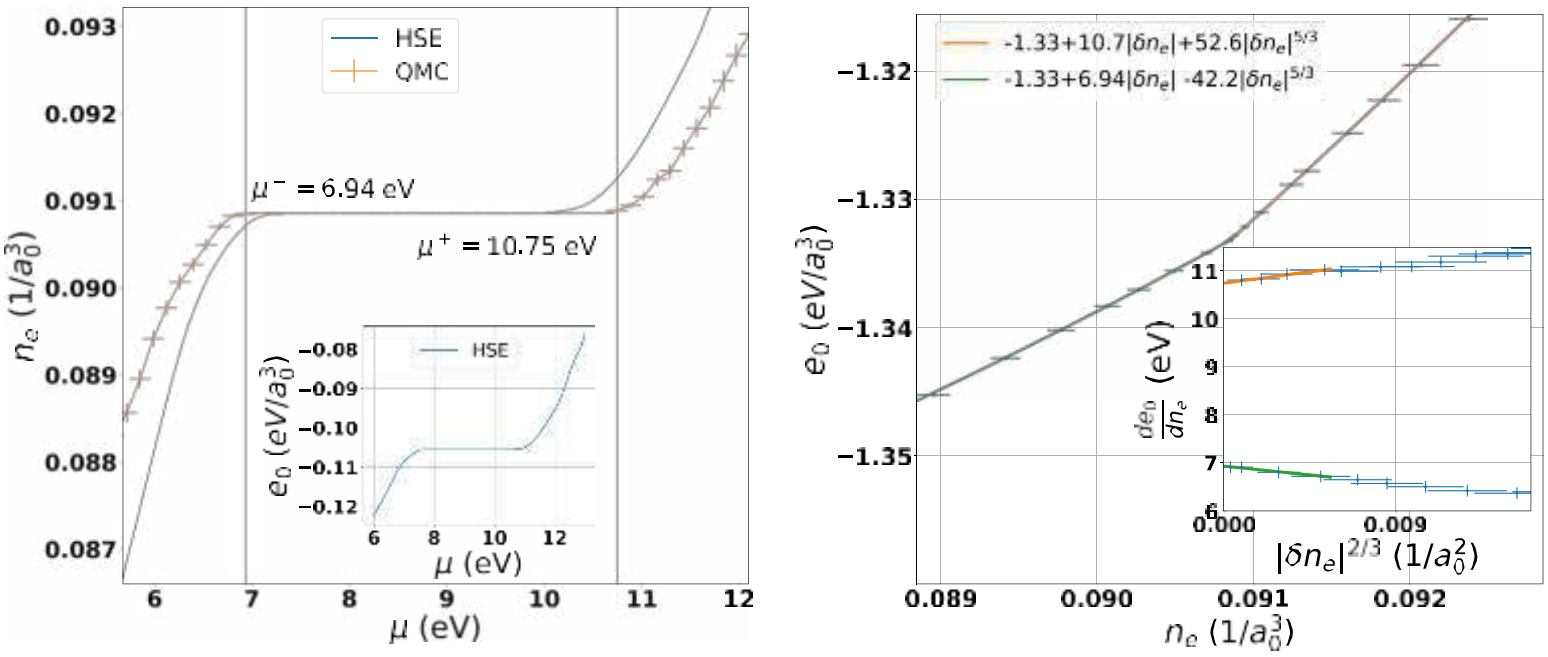

(a) (b)

FIG. 1. GCTABC analyses of the C2/c-24 structure of solid hydrogen at $r_s = 1.38$ (234GPa). (a) The electron density, n_e, as a function of the chemical potential μ obtained from HSE functional in comparison to QMC; the inset illustrates the energy density, e_0, as a function of μ from HSE functional. (b) Energy density, e_0, as a function of n_e using QMC; the inset shows the derivative discontinuity, where δn_e is the change of the electronic density with respect to the insulating state. Size corrections, as discussed in the text, are included.

Value of the gap can be extracted from the size of the incompressible region (plateau) or from the kink in the energy density at $n_e = n_p$

$$\Delta_{qp} = \mu^+ - \mu^- = \left.\frac{d\langle e_0\rangle_\theta}{d\langle \bar{n}\rangle_\theta}\right|_{n=0^+} - \left.\frac{d\langle e_0\rangle_\theta}{d\langle \bar{n}\rangle_\theta}\right|_{n=0^-}$$

Finite size effects (FSE): total energy

- Extended systems are considered in Periodic Boundary Conditions.
- Energy and other properties for the finite systems are affected by FS error that need to be understood and corrected in order to provide accurate results.
- Extrapolation to the infinite size system should be supported by a theoretically derived behaviour because an empirical brute force characterisation is often uncertain: often one cannot explore a wide range of sizes and it is not clear whether the asymptotic (power law) behaviour is already reached. Moreover the results will be dominated by the smallest size systems with smaller error bars.
- Empirical observed behaviours:
  $E(N) \sim 1/N \sim 1/L^3$ vs $E(N) \sim 1/N^{1/3} \sim 1/L$
- In this paper we studied in details the various corrections to the total energy

PHYSICAL REVIEW B **94**, 035126 (2016)

Theory of finite size effects for electronic quantum Monte Carlo calculations of liquids and solids

Markus Holzmann,[1,2,3] Raymond C. Clay III,[4] Miguel A. Morales,[5] Norm M. Tubman,[4] David M. Ceperley,[4] and Carlo Pierleoni[6]

Two types of contributions:

- single electron contributions are treated by twisted boundaries (averaging over) and by Grandcanonical calculations
- two-electron contributions are encoded in the small-k behavior of the el-el structure factor $S_{ee}(k \to 0)$
- corrected energies are closed to convergence already for 100 electrons in metallic hydrogen (~ 0.5 mH/el)

Size correction for gaps (#1)

- As for the total energy, single electron size effects are corrected by TABC.
- Two-particle size effects are encoded in the $S_{N_e \pm 1}(k \to 0)$.
- We proved that

$$S_k^{\pm} = (N_e \pm 1) S_{N_e \pm 1}(k) - N_e S_{N_e}(k) \sim \alpha_{\pm} + O(k^2); \qquad \alpha_{\pm} \propto \pm \epsilon_{k \to 0}^{-1}$$

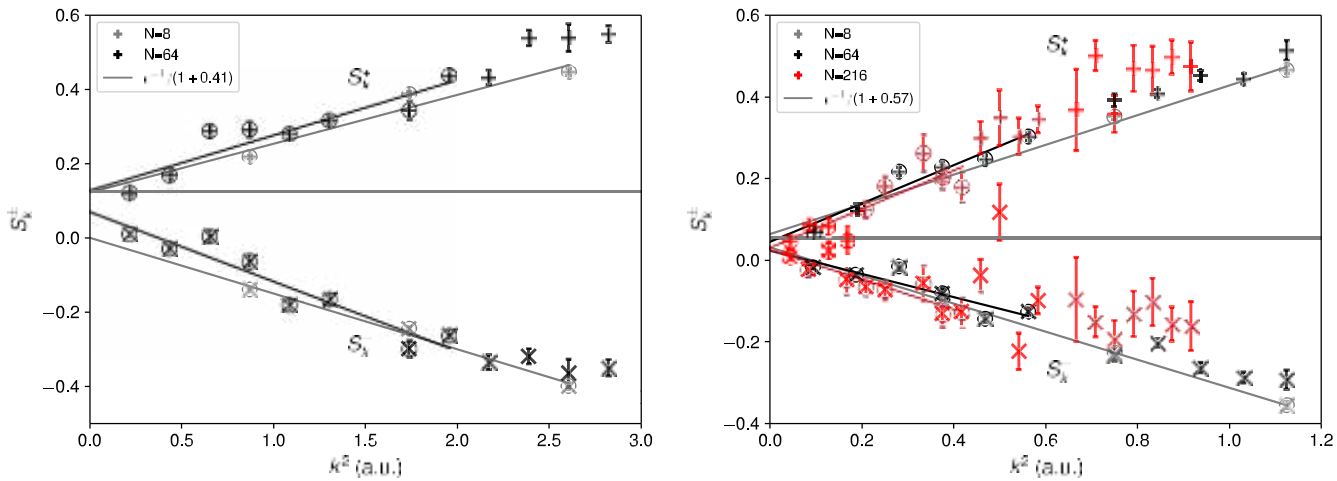

(a) carbon (b) silicon

FIG. 2. Change in the static structure factor as an electron (upper curves) or a hole (lower curves) is added to the insulating system with N atoms. The lines are fits to the data points. The horizontal lines show the expected $k \to 0$ limit based on the experimental dielectric constants. We have used $c = 0.41$ for C and $c = 0.57$ for Si.

- Potential energy correction to the gap: $\Delta_{\Delta_e} \simeq \pm \alpha \frac{|v_M|}{2} \sim \frac{1}{L}$; v_M = Madelung constant $\sim \frac{1}{L} \sim \frac{}{N}$
- Kinetic energy correction from correlations: $\Delta'_{\Delta e} \simeq \alpha_{\pm} c \frac{|v_M|}{2}$
- Total correction: $\Delta_\infty - \Delta_V \simeq \frac{|v_M|}{\epsilon_{k \to 0}} + O\left(\frac{1}{V}\right)$

Size correction for gaps (#2)

Next to leading order corrections $\delta\Delta_s^N$ comes from twists corrections to two-particle correlations. This are unessential for total energies, but important for the gaps since gaps values are of the order of total energies corrections for the system sizes under considerations.

TABLE I. Energy gaps obtained from GCTAB QMC in eV. The bare gap, ω_N, was calculated from Eq. (1) for a finite supercell containing N atoms. The leading-order finite-size corrections are given by the screened Madelung constants $|v_M|/\epsilon$, the next-to-leading order by the twist correction of two-particle density correlations, $\delta\omega_s$. We used the experimental value of ϵ for C and Si (5.7 and 11.7, respectively) and the value 18.8 for H_2 extracted from S(k). Finite-size corrections were also applied to the band edges, $\mu^{\pm}$. The estimate of the gap in the thermodynamic limit is $\omega_\infty = \omega_{N_e} + |v_M|/\epsilon + \delta\omega_s$. From our LDA analysis, we estimate a systematic bias of ~0.1 eV from the finite twist grid. This bias is larger than the statistical error. SJ indicates Slater-Jastrow trial wave function, while BF indicates backflow. The lattice constants of carbon and silicon are 3.567 Å and 5.43 Å, respectively.

	r_s	N	ω_N	$\lvert v_M\rvert/\epsilon$	$\delta\omega_s$	μ^-_∞	μ^+_∞	ω_∞
H_2 (BF)	1.38	96	3.3(1)	0.40	0.020	6.9(1)	10.7(1)	3.8(1)
	1.34	96	2.4(1)	0.20	0.018	8.6(1)	11.2(1)	2.6(1)
C (BF)	1.318	8	3.9(1)	2.01	0.69	11.5(1)	18.1(1)	6.6(1)
C (SJ)	1.318	8	4.0(1)	2.01	0.69	11.5(1)	18.2(1)	6.7(1)
		64	5.8(1)	1.00	0.02	11.9(1)	18.7(1)	6.8(1)
Si (BF)	2.005	8	0.6(1)	0.64	0.55	5.2(1)	6.9(1)	1.7(1)
Si (SJ)	2.005	8	0.6(1)	0.64	0.58	5.2(1)	7.0(1)	1.9(1)
		64	1.4(1)	0.32	0.08	5.5(1)	7.3(1)	1.8(1)
		216	1.6(1)	0.21	0.01	5.6(1)	7.4(1)	1.8(1)

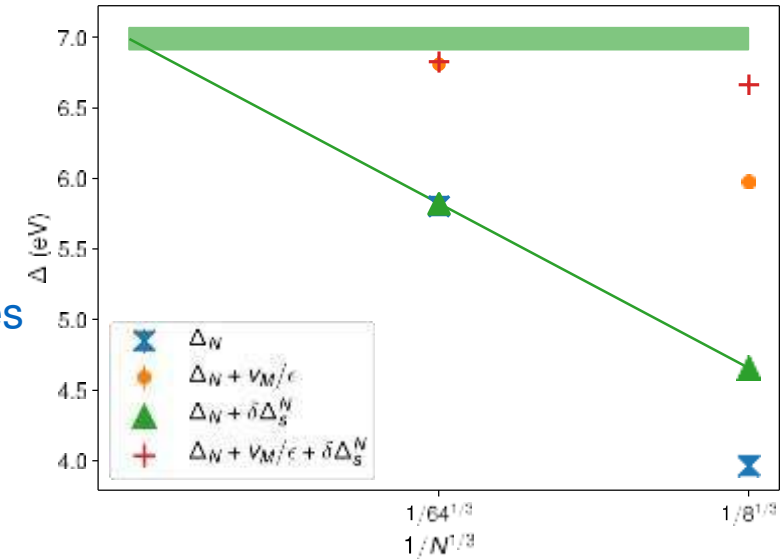

(a) carbon

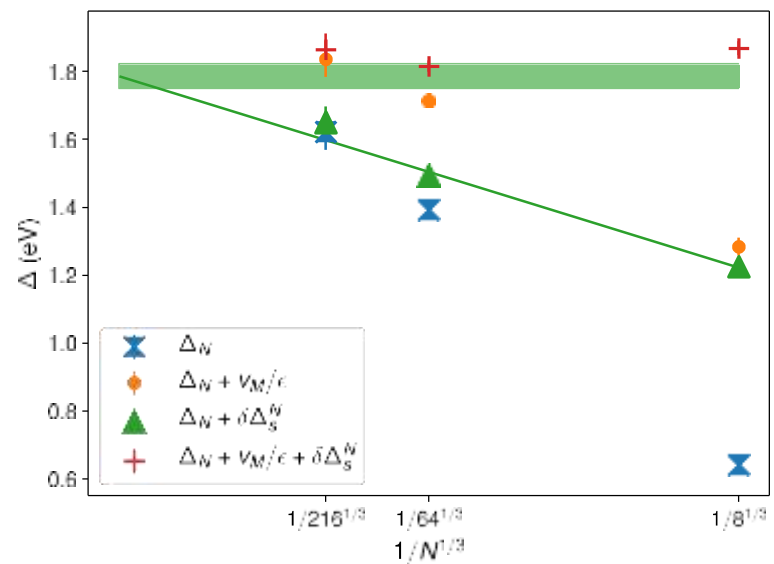

(b) silicon

FIG. 4. Fundamental gap before and after finite-size corrections. ω_N is the DMC gap from a simulation with N atoms in the supercell without any finite-size correction, v_M/ϵ is the leading-order Madelung correction using the experimental value of ϵ^{-1}, $\delta\omega^N{}_s$ is the next-to-leading-order density correction, which is related to the static part of the structure factor. The line is a fit to $\omega_N + \delta\omega_s^N$.

Comparison with experiments for Si and C

Our values are larger than experimental determinations:

TABLE II. Extrapolated band gap of Si and C from backflow DMC calculations, Δ_{BF} compared to the experimental values (exp). We tabulated two main corrections: the difference between the gap of an all-electron (AE) and the pseudopotential (PP) calculation within GW calculations, and the neglect of electron-phonon coupling (e-ph).

	Δ_{BF}	AE - PP	e-ph	exp
C	6.6(2)	-0.26 (G_0W_0) [54]	-0.6 (GW) [56]	5.48 [67]
Si	1.7(1)	-0.25 (G_0W_0)[54]	-0.06 (DFT) [57]	1.17 [67]

Pseudopotential effects and electron-phonons effects reduces the gap.

Comparison with experiment is not conclusive.

Hydrogen fundamental gap for ideal structures ($N_p = 96$)

V. Gorelov, M. Holzmann, DM Ceperley and C. Pierleoni, PRL **124**, 116401 (2020).

(structures optimized with vdW-DF)

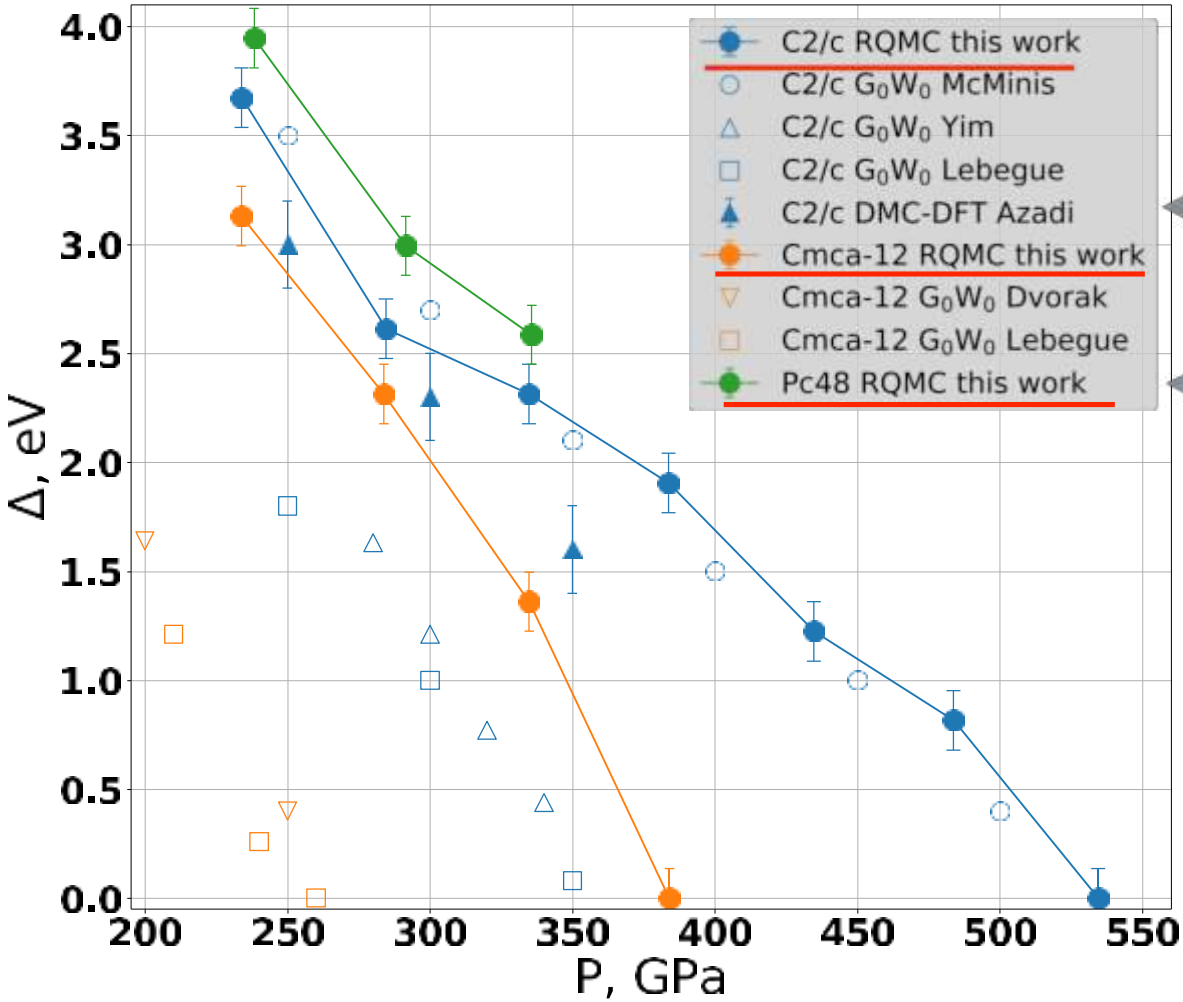

Phase III

QMC+scissor correction and size extrapolation (2018)

Phase IV

- Excellent agreement with GW gaps from McMinis (same structures)
- Good agreement with previous QMC estimates (Azadi et al, PRB 2017) but …
- other GW calculations predict smaller gap (1-2 eV smaller) but use different structural optimization.

Neutral (particle-hole) gap

V. Gorelov, Y. Yang, M. Ruggeri, D.M. Ceperley, C. Pierleoni and M. Holzmann, Cond. Mat. Phys. **26**, 33701 (2023).

- In an ideal crystal $\Psi_{\mathbf{k}}(\mathbf{r}_1 + \mathbf{t}, \mathbf{r}_2 + \mathbf{t}, \ldots, \mathbf{r}_{N_e} + \mathbf{t}) = e^{i\mathbf{k}\cdot\mathbf{t}}\Psi_{\mathbf{k}}(\mathbf{r}_1, \mathbf{r}_2, \ldots, \mathbf{r}_{N_e})$ $\mathbf{t}$ crystal symmetry
- Assuming the ground state is at $\mathbf{k} = \mathbf{0}$, any $\mathbf{k} \neq \mathbf{0}$ in the Brillouin zone is an excited state and

$$\Delta_n = \min_{\mathbf{k}\neq\mathbf{0}} E_{\mathbf{k}}(N_e) - E_0(N_e)$$

therefore, likewise the fundamental gap, even the neutral gap can be obtained from GS calculations with different crystal momentum. In the TL, $\mathbf{k}$ becomes a continuum and, for a normal band insulator, even the vertical gap could be obtained by extrapolation.

- With TABC, the twist is a second quantum number and eigenstates can be labeled by $\mathbf{k}, \theta$. The GS energy, using M_θ twists, is

$$e_0 = \frac{1}{M_\theta V}\sum_\theta E_{\mathbf{k}_\theta}(\theta, N_e)$$

$E_{\mathbf{k}_\theta}(\theta, N_e)$ = GS energy of a system at $\mathbf{k}_\theta$, corresponding to minimum of the GS energy at

- Extending the above definition, the neutral gap is obtained as

$$\Delta_n = \min_{\theta,\mathbf{q}\neq 0} [E_{\mathbf{k}_\theta+\mathbf{q}}(\theta, N_e) - E_{\mathbf{k}_\theta}(\theta, N_e)]$$

where $\mathbf{q}$ is a reciprocal space vector compatible with the twist grid (finite crystal momentum).

Example: Carbon diamond

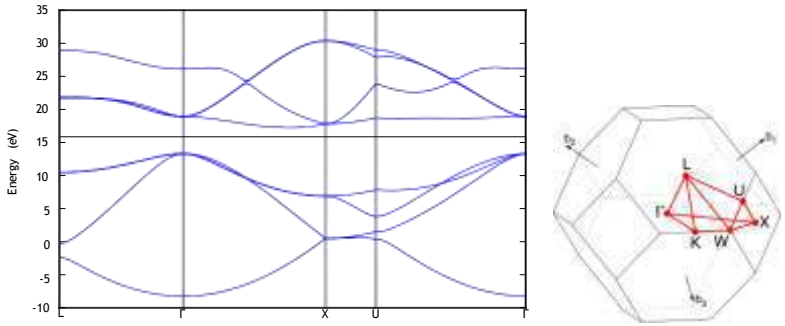

Figure 1. (Colour online) Left-hand: DFT-LDA band structure of carbon diamond. Right-hand: Brillouin zone of diamond structure with the selected path for band structure plot.

Table 1. Neutral gap, Δ_n from DMC calculations of carbon diamond in a supercell containing N = 8 and 64 atoms for Γ – X and Γ – Γ transitions, compared to the corresponding quasiparticle band gaps Δ_{QP} from [14].

N	**k**	$\Delta_n(\mathbf{k})$	$\Delta_{QP}(\mathbf{k})$
8	Γ → X	4.565(6)	4.59(2)
	Γ → Γ	6.265(6)	
64	Γ → X	6.04(2)	5.98(4)
	Γ → Γ	7.64(2)	

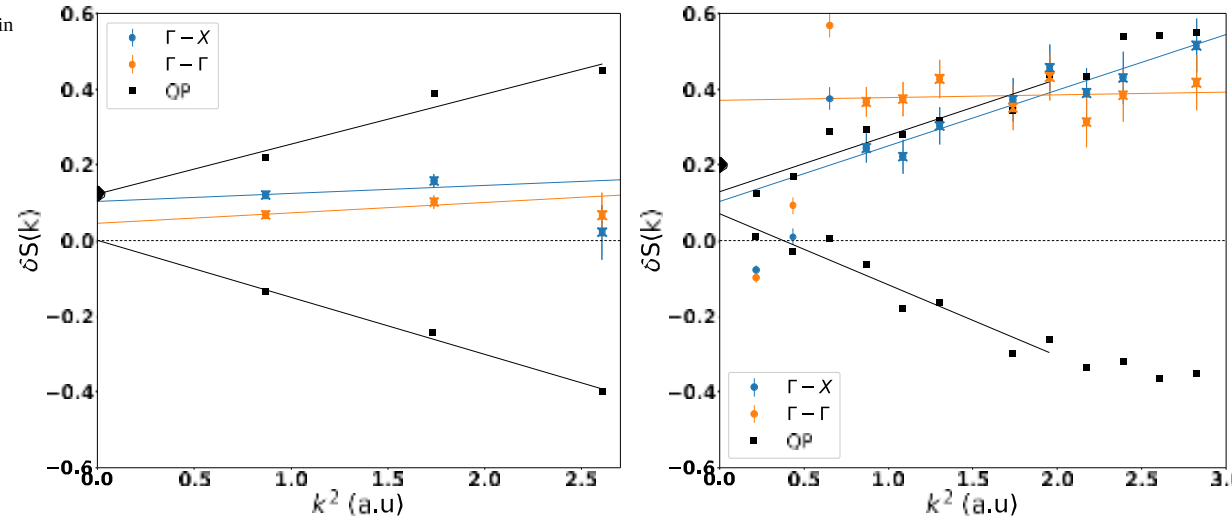

Figure 2. (Colour online) Difference between the excited and ground state fluctuating structure factor for carbon, $\delta S(\mathrm{k})$. Blue and orange: neutral excitations for Γ – X and Γ – Γ. Black: difference of structure factors from quasiparticle excitations for addition, $\delta S^{+}(\mathrm{k})$, (upper branch) and removal, $\delta S^{-}(\mathrm{k})$, (lower branch) from [14]. Left-hand: 8 atoms, right-hand: 64 atoms. The lines are fits to the data points of the corresponding color. Symbols with crosses are included in the fit. From our anaytical analysis, we expect $\delta S(\mathrm{k}) \approx \delta S^{+}(\mathrm{k}) + \delta S^{-}(\mathrm{k})$ for $\mathrm{k} \to 0$. Values for small k are likely affected by a larger uncertainty, in particular for the larger system. Dotted horizontal lines indicate zero.

- Finite size effects are similar to the fundamental gap if excitation are represented by extended DFT orbitals

$$\Delta_n(\infty) - \Delta_n(\mathrm{L}) \simeq \frac{|v_M|}{\epsilon} \sim \frac{1}{\mathrm{L}}$$

- Exciton localization can only be obtained by more complex wave functions. If ℓ_X represent the exciton localisation length, we expect negligible size effect ($\sim 1/\mathrm{N}$) for $\mathrm{L} \geq 2\ell_X$.

- a sign of this will be in $\delta S(\mathrm{k} \to 0) = 0$

Thermal and quantum crystals

Gorelov, Holzmann, Ceperley and Pierleoni, PRL **124**, 116401 (2020)
Gorelov, Ceperley, Holzmann and Pierleoni, J. Chem Phys. **153**, 234117 (2020)

We need to include nuclear effects such as zero-point and thermal motion.
Zero-point effects (quantum nuclei) are essential for hydrogen.
Both effects are treated by representing nuclei (protons) by Feynman Path Integrals in imaginary time.
In the canonical ensemble we write

$$Z(N_e) = e^{-\beta F(N_e)} = \int \mathcal{D}\mathbf{R}(\tau) e^{-S[\mathbf{R}(\tau)]}$$

where the action is defined as

$$S[\mathbf{R}(\tau)] = \int_0^\beta d\tau \left[\frac{\hbar^2}{2M} \left(\frac{d\mathbf{R}(\tau)}{d\tau} \right)^2 + E_0(\mathbf{R}(\tau), N_e) \right]$$

$\mathbf{R}(\tau)$ are the proton positions and $E_0(\mathbf{R}(\tau), N_e)$ the BO energy for the system with N_p protons and N_e electrons.

When $N_e \neq N_p$, we have

$$\frac{Z(N_e)}{Z(N_p)} = e^{-\beta[F(N_e)-F(N_p)]} = \left\langle e^{-\int_0^\beta d\tau \delta E_0(\mathbf{R}(\tau),N_e)} \right\rangle ; \qquad \delta E_0(\mathbf{R}, N_e) = E_0(\mathbf{R}, N_e) - E_0(\mathbf{R}, N_p)$$

When

$$|N_e - N_p| \ll N_p \Longrightarrow |\delta E_0(\mathbf{R}, N_e)| \ll |E_0(\mathbf{R}, N_p)| \Longrightarrow F(N_e) - F(N_p) \simeq \langle \delta E_0(\mathbf{R}(0), N_e) \rangle - \frac{\sigma^2(N_e)}{2}$$

with

$$\sigma^2(N_e) = \int^\beta d\tau \langle \delta E_0(\mathbf{R}(\tau), N_e) \delta E_0(\mathbf{R}(0), N_e) \rangle_c$$

Adding or removing a single electron, we obtain the chemical potential from the free energy differences

$$\mu^{\pm} = \pm \left[F(N_p \pm 1) - F(N_p) \right] \Longrightarrow \Delta_{qp} = \mu^{+} - \mu^{-}$$

hence the terms $\sigma^2(N_p \pm 1)$ contributes with opposite sign to the gap and largely cancels providing

$$\Delta_{qp} \simeq \langle \delta E_0(N_p + 1) \rangle - \langle \delta E_0(N_p - 1) \rangle$$

In practice we need to replace the ground state energy density for the ideal crystal with the average internal energy density for the thermal and quantum crystal

$$\Delta_{qp} = \mu^{+} - \mu^{-} \simeq \left. \frac{du(\bar{n}(\mu))}{d\bar{n}(\mu)} \right|_{0^+} - \left. \frac{du(\bar{n}(\mu))}{d\bar{n}(\mu)} \right|_{0^-}$$

Gap reduction by NQE (and temperature) in high pressure hydrogen

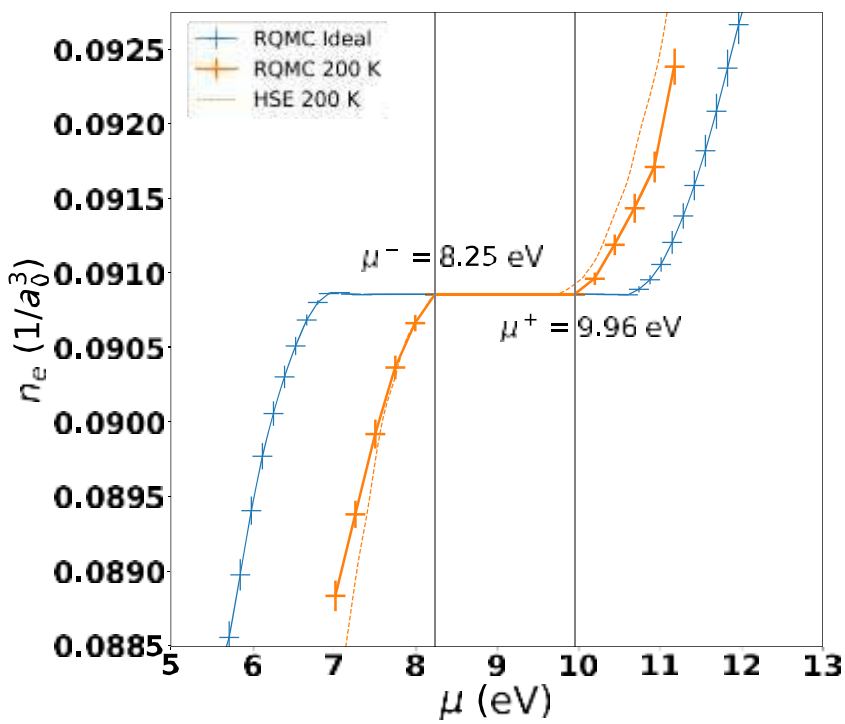

FIG. 4. Mean electron density from QMC-CEIMC calculations (orange solid line) and the integrated DOS computed with the HSE density functional (orange dashed line) for the C2/c-24 hydrogen crystal at 248 GPa and 200 K plotted together with the RQMC electron density for a perfect hydrogen crystal (blue line).

Hydrogen phase diagram

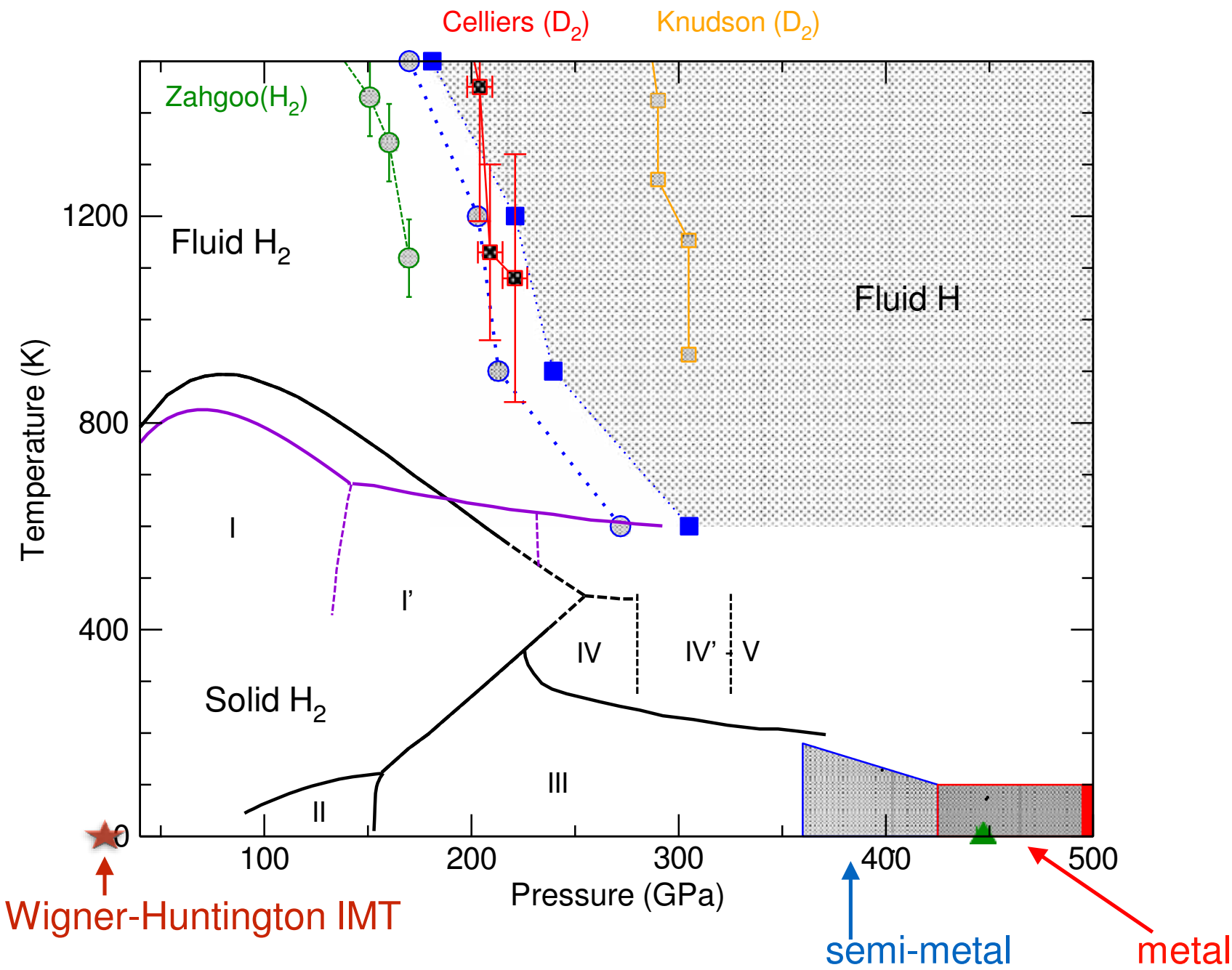

CP in L. Boeri et al, J. Phys. Cond. Mat. ***34****, 183002 (2022)*

Experimental evidence of hydrogen metallization

Science 355, 715–718 (2017) 17 February 2017

Observation of the Wigner-Huntington transition to metallic hydrogen

Ranga P. Dias and Isaac F. Silvera*

Reflectivity

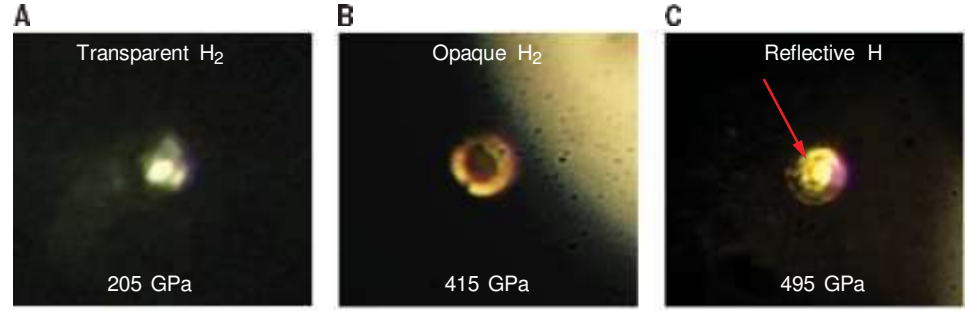

Semimetallic molecular hydrogen at pressure above 350 GPa

M. I. Eremets*, A. P. Drozdov, P. P. Kong and H. Wang

Nature Physics (2019)

electrical conductivity measurements

Synchrotron infrared spectroscopic evidence of the probable transition to metal hydrogen

P. Loubeyre, F. Occelli and P Dumas

Nature | Vol 577 | 30 January 2020 | 631

Infrared absorption

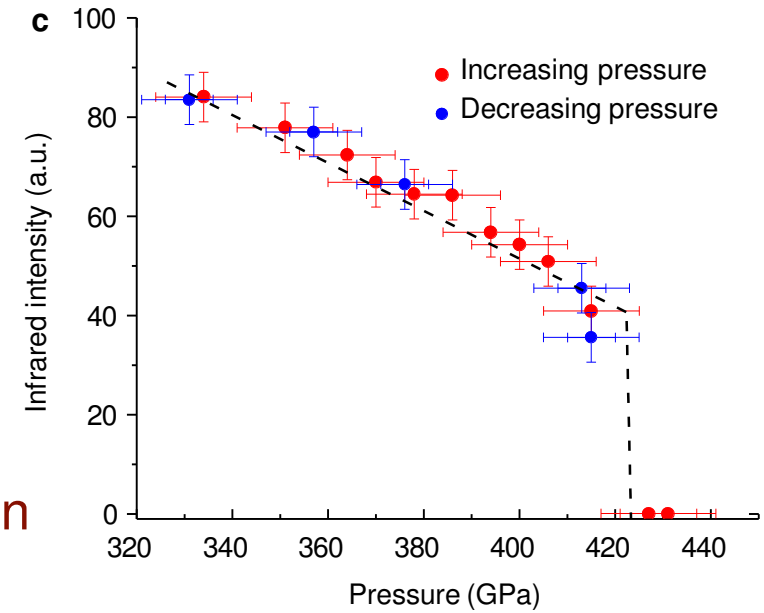

Inelastic X-ray spectroscopy T=300K; 5GPa < P < 90GPa

Probing the Electronic Band Gap of Solid Hydrogen by Inelastic X-Ray Scattering up to 90 GPa

PHYSICAL REVIEW LETTERS 126, 036402 (2021)

Bing Li,[1] Yang Ding,[1] Duck Young Kim,[1] Lin Wang,[1,2] Tsu-Chien Weng,[1,3,*] Wenge Yang [1] Zhenhai Yu,[1] Cheng Ji [1,4] Junyue Wang,[1] Jinfu Shu,[1] Jiuhua Chen,[5] Ke Yang,[6] Yuming Xiao,[4] Paul Chow,[4] Guoyin Shen [4] Wendy L. Mao,[7,8] and Ho-Kwang Mao[1,†]

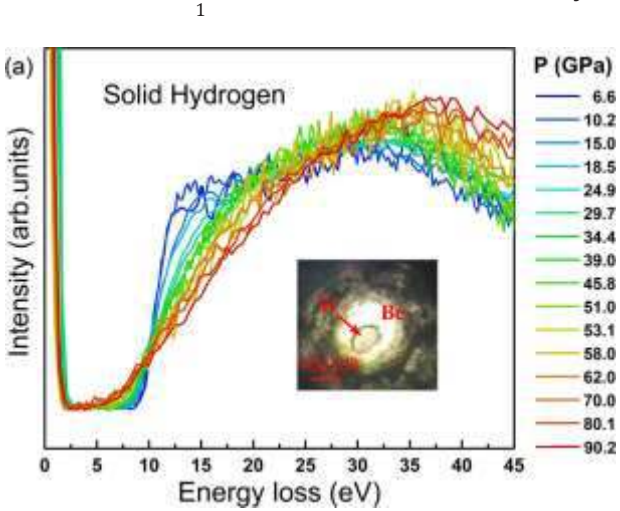

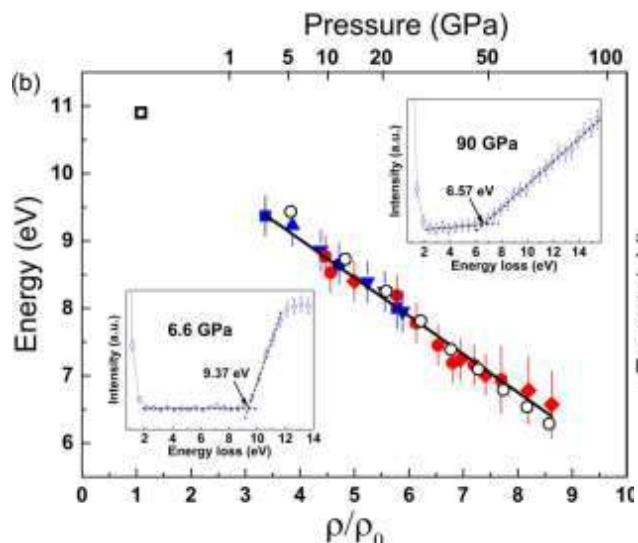

FIG. 3. (a) IXS spectra of solid hydrogen at high pressures from 6.6 to 90.2 GPa. The inset photomicrograph shows the 100 μm hydrogen sample at 90.2 GPa. (b) The band gap of solid hydrogen determined at the breaking points of the slopes of the IXS spectra (illustrated in the insets); blue, experiments at APS; red, experiments at SSRF; seven different solid symbols represent separate DAC IXS experiments; open square, the zero pressure ($<10^{-7}$ torr), low temperature (2 K) threshold energy from Ref. [11]; open circles, theoretical calculations; solid line, linear regression of the IXS experimental data.

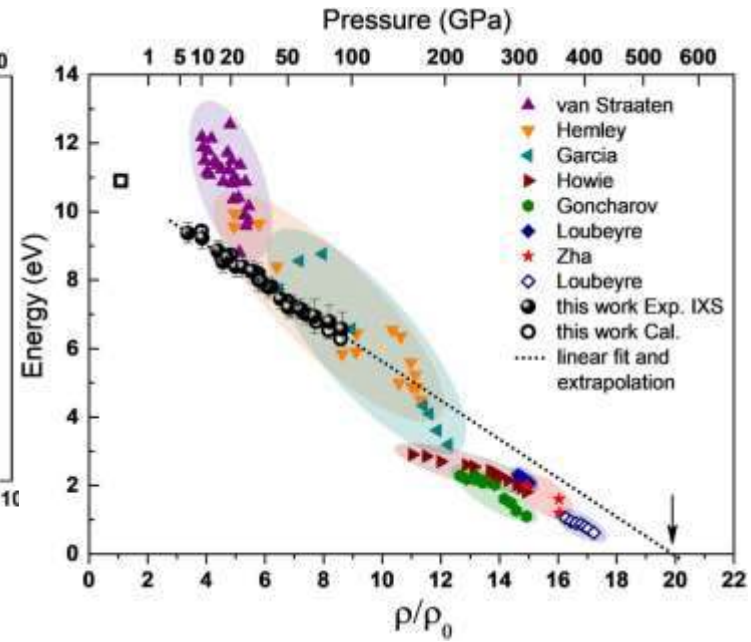

FIG. 4. Threshold energy of solid hydrogen from IXS as a function of density and pressure. The open square corresponds to the zero pressure ($<10^{-7}$ torr), low temperature (2 K) threshold energy from Ref. [11]. Open circles represent the data from theoretical calculations in this work. Filled black circles are IXS data from this work compared with experimental data from Van Straaten [12] (upward triangles), Hemley [13] (downward triangles), Garcia [14] (left triangles), Howie [15] (right triangles), Goncharov [16] (hexagons), Loubeyre [17] (diamonds), Zha [18] (stars), and Loubeyre [6] (open diamonds). The shade areas show the scattering of the data set with the same color hues. The dotted line shows the trend of band-gap closure as a guide for the eye.

Open circles — theoretical calculations:

1) *P6₃/m* structure optimized with DFT-BLYP
2) Band structure from DFT-HSE06
3) nuclear thermal and quantum effects neglected
4) but molecules in phase I rotates !!!

Trial wave functions for hydrogen

- In the fixed node approximation, the accuracy depends on the form of the many body trial wave function.
- Slater-Jastrow form: $\Psi_T(R|S) = \exp[-U(R|S)]\ \mathrm{Det}\ \Sigma^{\uparrow}\ \ \mathrm{Det}\ \Sigma^{\downarrow}$
- U(R|S) is a (one-body + two-body + three-body + ...) correlation factor (bosonic).
- $\sum$ is a Slater determinant of single electron orbitals $\theta_k(\vec{x}_i, \sigma_i|S)$
- The nodes are determined by the form of the orbitals only. They are the most important part of the trial function since the nodes are not optimized by projection.

- Hydrogen trial function
  - Single electron orbitals from DFT (with various approxs) for each proton configuration.
  - Analytical electron-electron and electron-proton backflow transformation (BF) to improve the nodes [Holzmann, Ceperley, Pierleoni, Esler PRE 68, 046707 (2003)].
  - Analytical form for the 1-body and 2-body Jastrow from RPA (Gaskell, 1967)
  - Addition of numerical 1-body, 2-body, 3-body Jastrows and backflow terms
  - few variational parameters to be optimized (on selected configurations only).

13 variational parameters only ! effect of optimization: ~1 mH/at on the energy
~40% on the variance

Hydrogen phase diagram

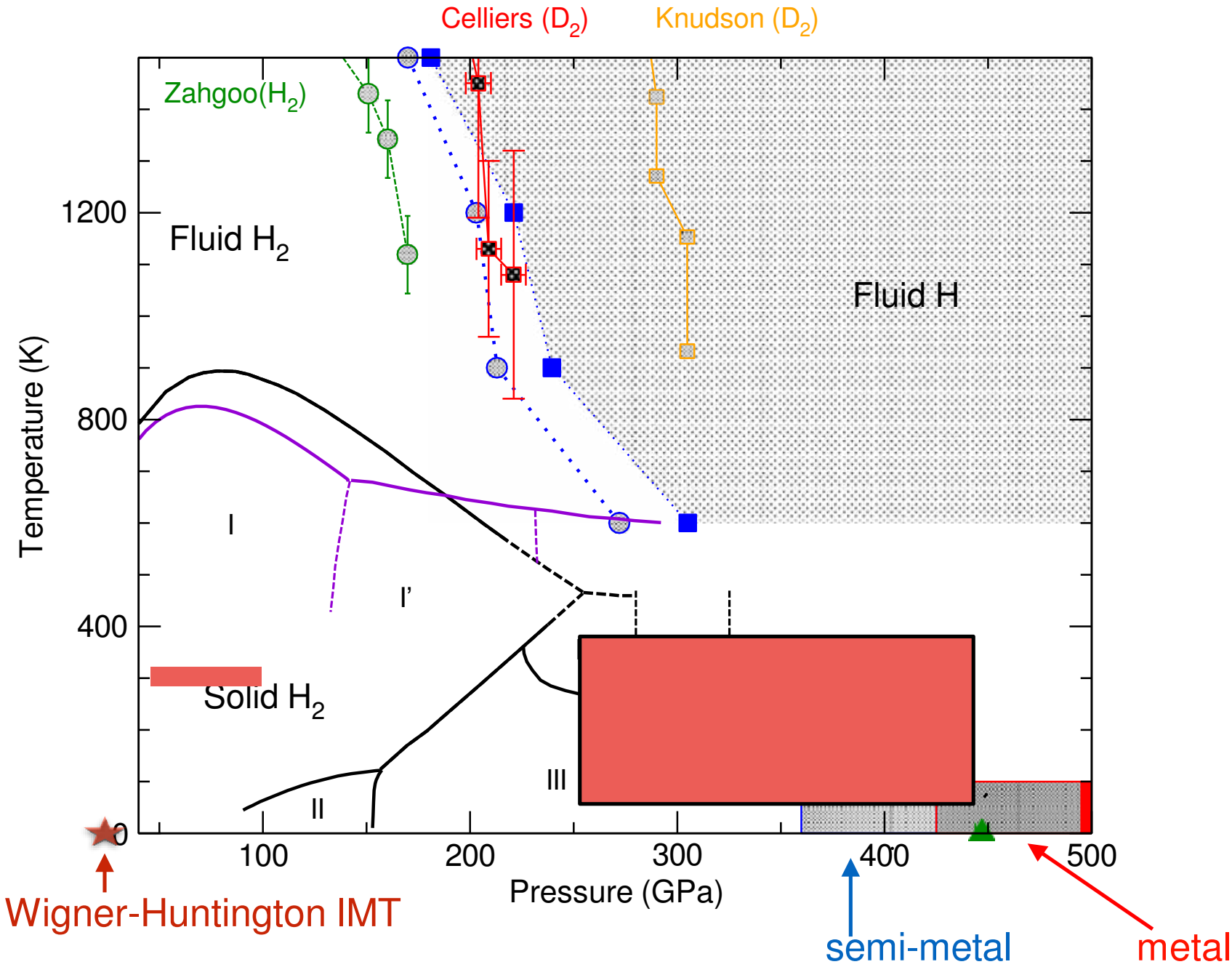

CP in L. Boeri et al, J. Phys. Cond. Mat. ***34****, 183002 (2022)*

Melting of Phase I up to 200GPa

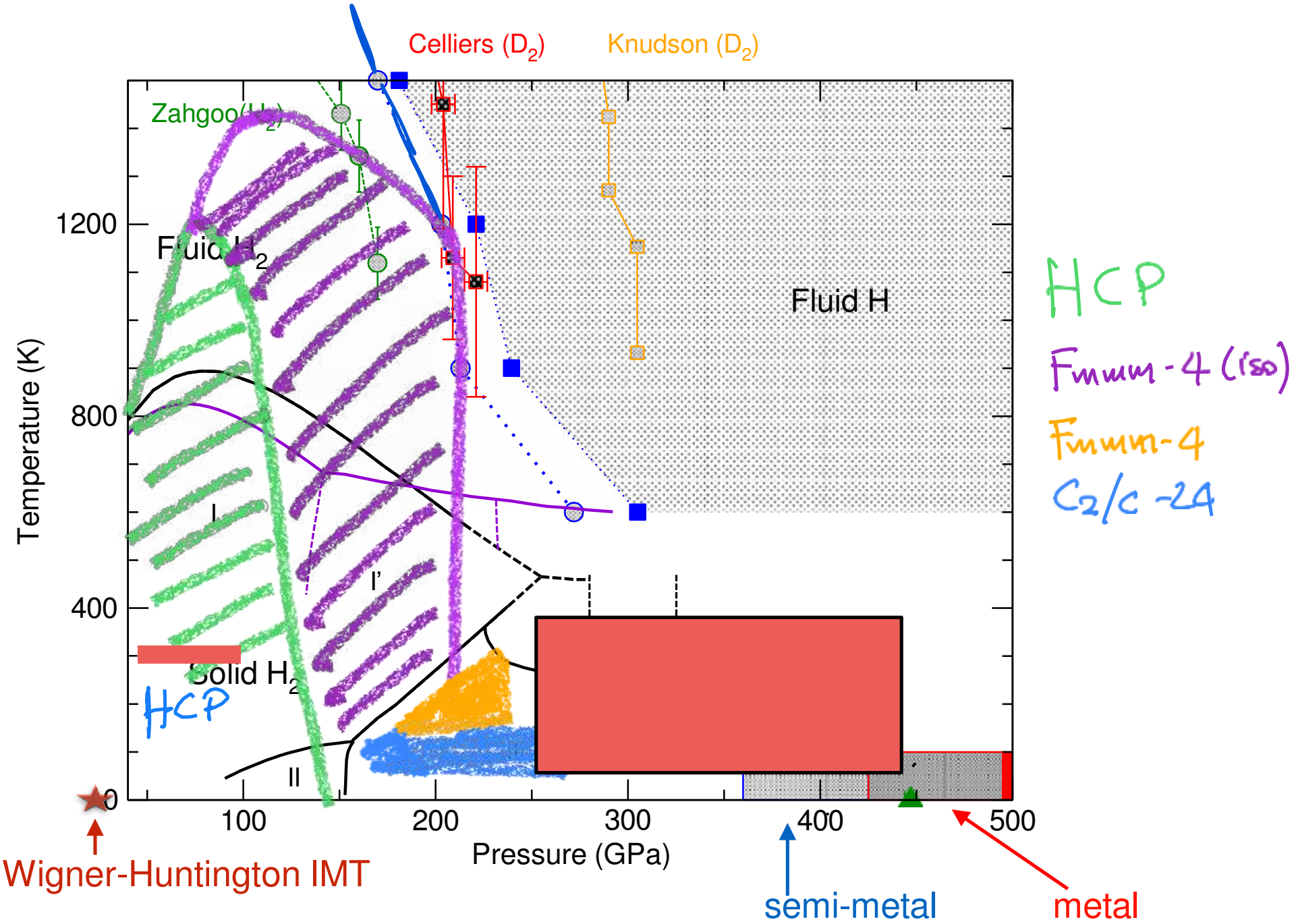

*Hongwei Niu et al, PRL **130**, 076102 (2023): modified phase diagram with QMC trained Machine Learning effective potential*

Nuclear quantum and thermal effects on the fundamental gap of H

thermal crystals

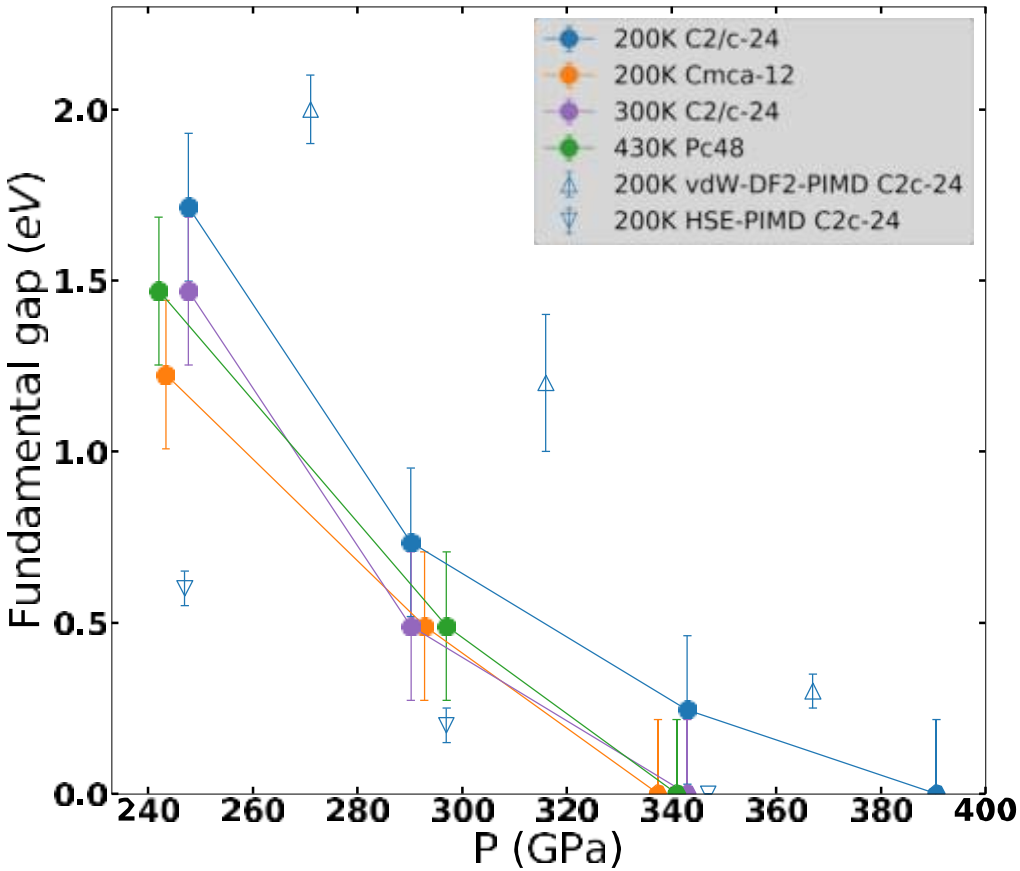

Ideal crystals

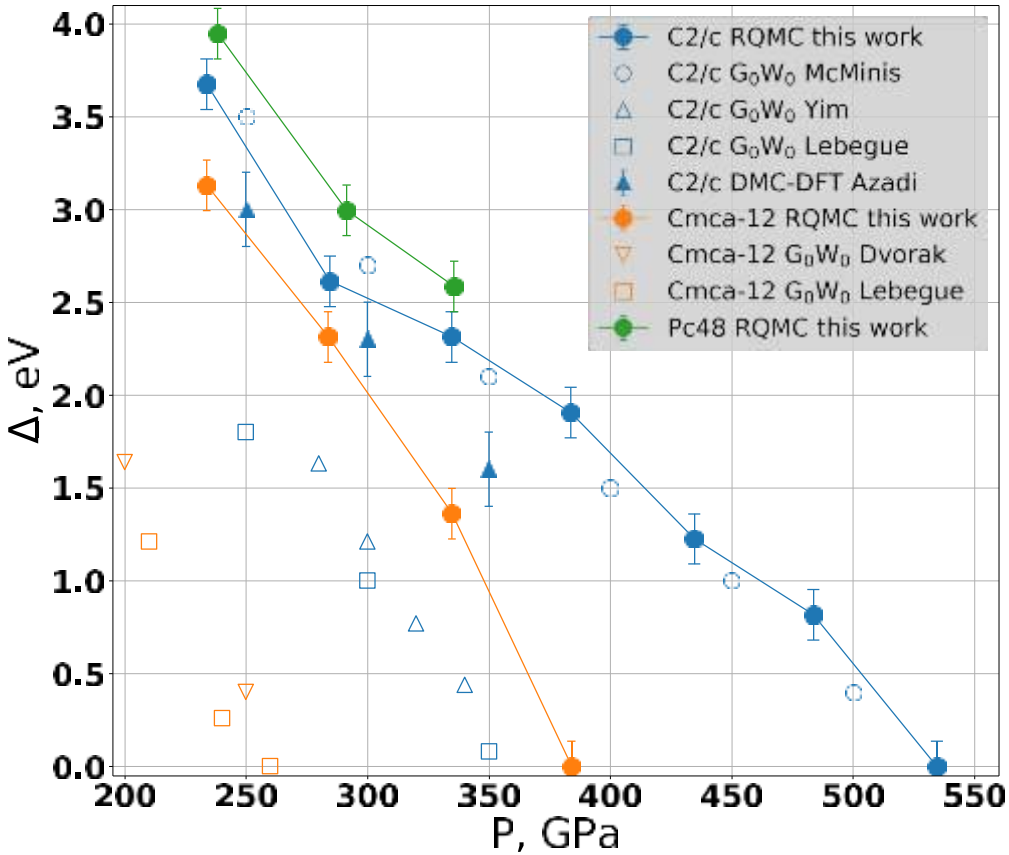

- The fundamental gap closes between 340GPa and 380GPa, depending on structure and temperature (temperature dependence is small).
- The gap reduction (~2-2.5eV) mainly comes from nuclear quantum effects.
- Qualitative agreement with experiments finding semi-metal at 360GPa (Eremets 2019).
- PIMD-vdW-DF2 is less “metallic” than QMC, while PIMD-HSE is more “metallic”(Morales 2013).

QMC gaps: comparison with experiments

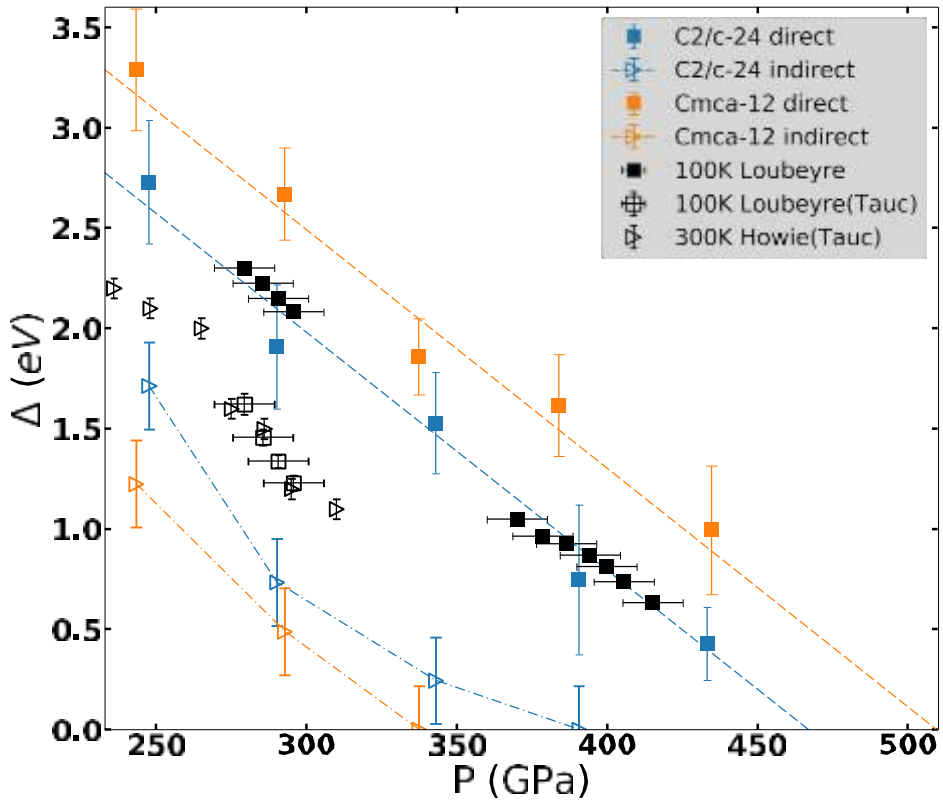

- Experimental indirect-gaps from **Tauc analysis** are slightly larger than our predictions.
- Experimental **direct gap** is associated with the complete infrared adsorption
- Loubeyre's latest experiment claims an abrupt collapse of the **direct gap** at 425GPa which is reversible upon releasing pressure.
- We cannot discuss this since our structures from CEIMC are dynamically stable.
- Excellent agreement for the direct gap, for C2/c-24 structure
- Recente work by Monacelli et al. based on the SSCHA (and QMC corrections) suggests that the observed absorption is related to a structural transition to a metallic Cmca12 structure.

Inelastic X-ray spectroscopy T=300K; 5GPa < P < 90GPa

Probing the Electronic Band Gap of Solid Hydrogen by Inelastic X-Ray Scattering up to 90 GPa

PHYSICAL REVIEW LETTERS 126, 036402 (2021)

Bing Li,[1] Yang Ding,[1] Duck Young Kim,[1] Lin Wang,[1,2] Tsu-Chien Weng,[1,3,*] Wenge Yang [1] Zhenhai Yu,[1] Cheng Ji [1,4] Junyue Wang,[1] Jinfu Shu,[1] Jiuhua Chen,[5] Ke Yang,[6] Yuming Xiao,[4] Paul Chow,[4] Guoyin Shen [4] Wendy L. Mao,[7,8] and Ho-Kwang Mao[1,†]

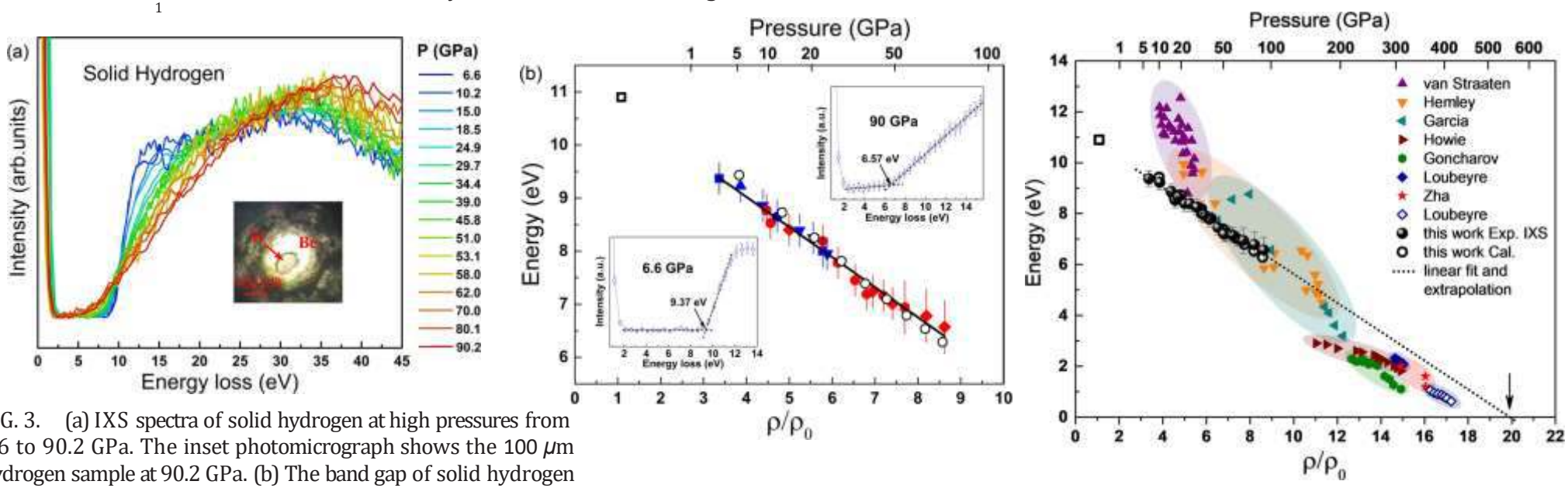

FIG. 3. (a) IXS spectra of solid hydrogen at high pressures from 6.6 to 90.2 GPa. The inset photomicrograph shows the 100 μm hydrogen sample at 90.2 GPa. (b) The band gap of solid hydrogen determined at the breaking points of the slopes of the IXS spectra (illustrated in the insets); blue, experiments at APS; red, experiments at SSRF; seven different solid symbols represent separate DAC IXS experiments; open square, the zero pressure ($<10^{-7}$ torr), low temperature (2 K) threshold energy from Ref. [11]; open circles, theoretical calculations; solid line, linear regression of the IXS experimental data.

FIG. 4. Threshold energy of solid hydrogen from IXS as a function of density and pressure. The open square corresponds to the zero pressure ($<10^{-7}$ torr), low temperature (2 K) threshold energy from Ref. [11]. Open circles represent the data from theoretical calculations in this work. Filled black circles are IXS data from this work compared with experimental data from Van Straaten [12] (upward triangles), Hemley [13] (downward triangles), Garcia [14] (left triangles), Howie [15] (right triangles), Goncharov [16] (hexagons), Loubeyre [17] (diamonds), Zha [18] (stars), and Loubeyre [6] (open diamonds). The shade areas show the scattering of the data set with the same color hues. The dotted line shows the trend of band-gap closure as a guide for the eye.

Open circles — theoretical calculations:

1) *$P6_3/m$* structure optimized with DFT-BLYP
2) Band structure from DFT-HSE06
3) nuclear thermal and quantum effects neglected
4) but molecules in phase I rotates !!!

Cristalline hydrogen in Phase I: QMC and MBPT (GW-BSE)

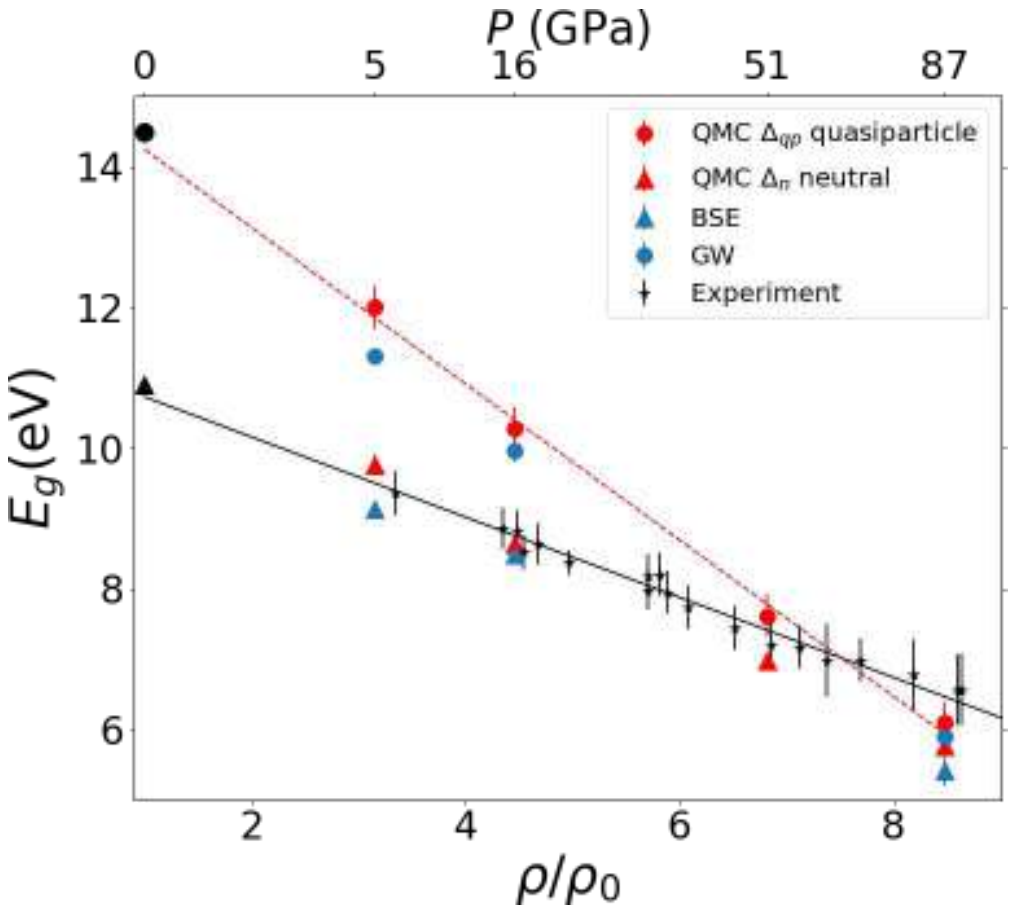

FIG. 1. Comparison between room temperature experimental data of ref. [16] and theoretical predictions for the electronic gap of solid hydrogen in phase I as a function of compression. We report quasi-particle (circles) and neutral gap from QMC (triangles) (red symbols) and from MBPT (blue symbols, circles GW, triangle BSE) both corrected for finite size e↵ects. The di↵erence between the quasi-particle and neutral gap is the exciton binding energy. The solid black line is a fit to experimental data; the red dashed line to QMC-QP gaps.

Reference values for zero pressure are from
Inoue et al., 1979 as cited by
Loubeyre et al, 2002

- triangle is a molecular excitation
- circle an interband transition

- At low compression neutral and QP gaps differ, the former agreeing with experiments, the latter extrapolating to the interband transition at ρ_0.
- At higher compression the two gaps are much closer and agree well with experiments (possible exp bias).
- In general good agreement between QMC and BSE gaps.
- Size effects are different at low and high compressions.

Inverse dielectric function from BSE calculations: comparison with experiments

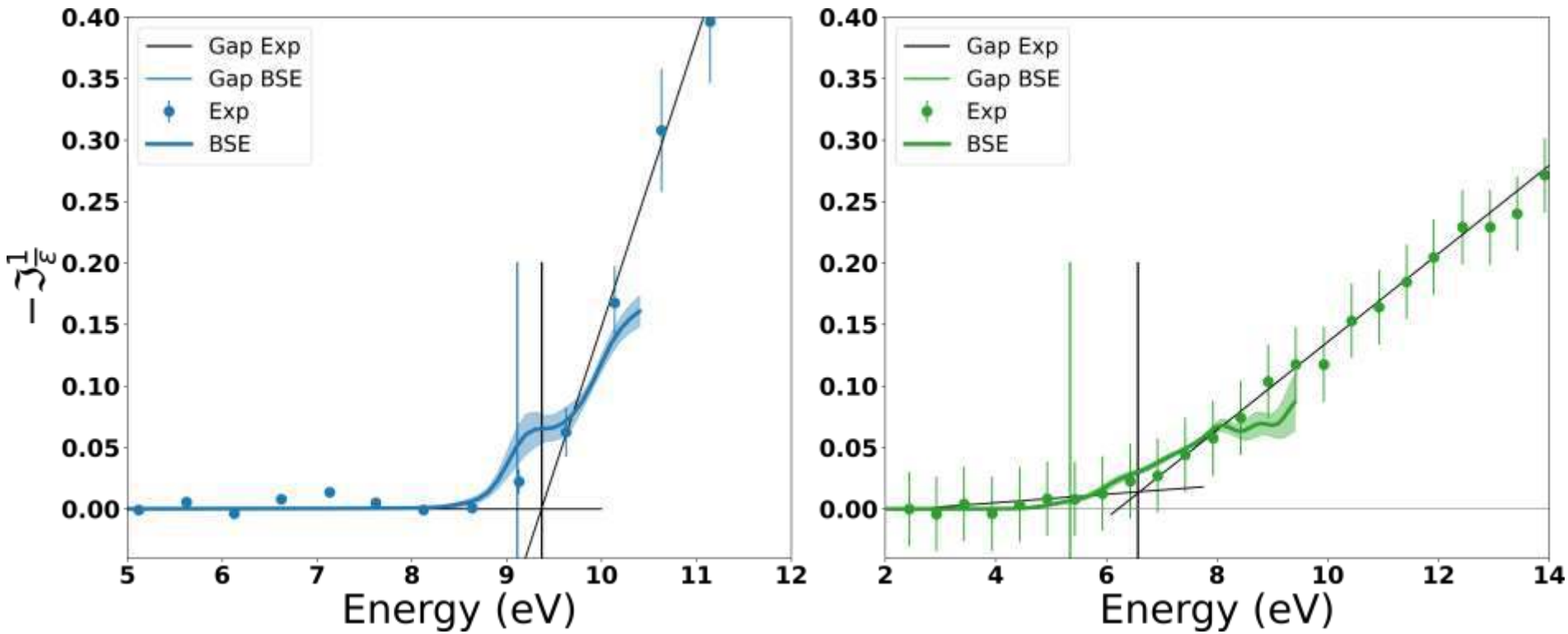

FIG. 2. Left - 5 GPa. Right - 90 GPa. Comparison of the measured and calculated with BSE IXS spectra for lowest and highest pressures. Vertical black lines indicate the band gap extracted from the measured spectra by fitting the onset (see other black lines). The vertical colored lines correspond to the calculated with the BSE neutral gap (we have verified that the poles of χ and $\bar{\chi}$ are identical) Only converged parts of the BSE spectra are shown.

Absorption profile: GW vs BSE

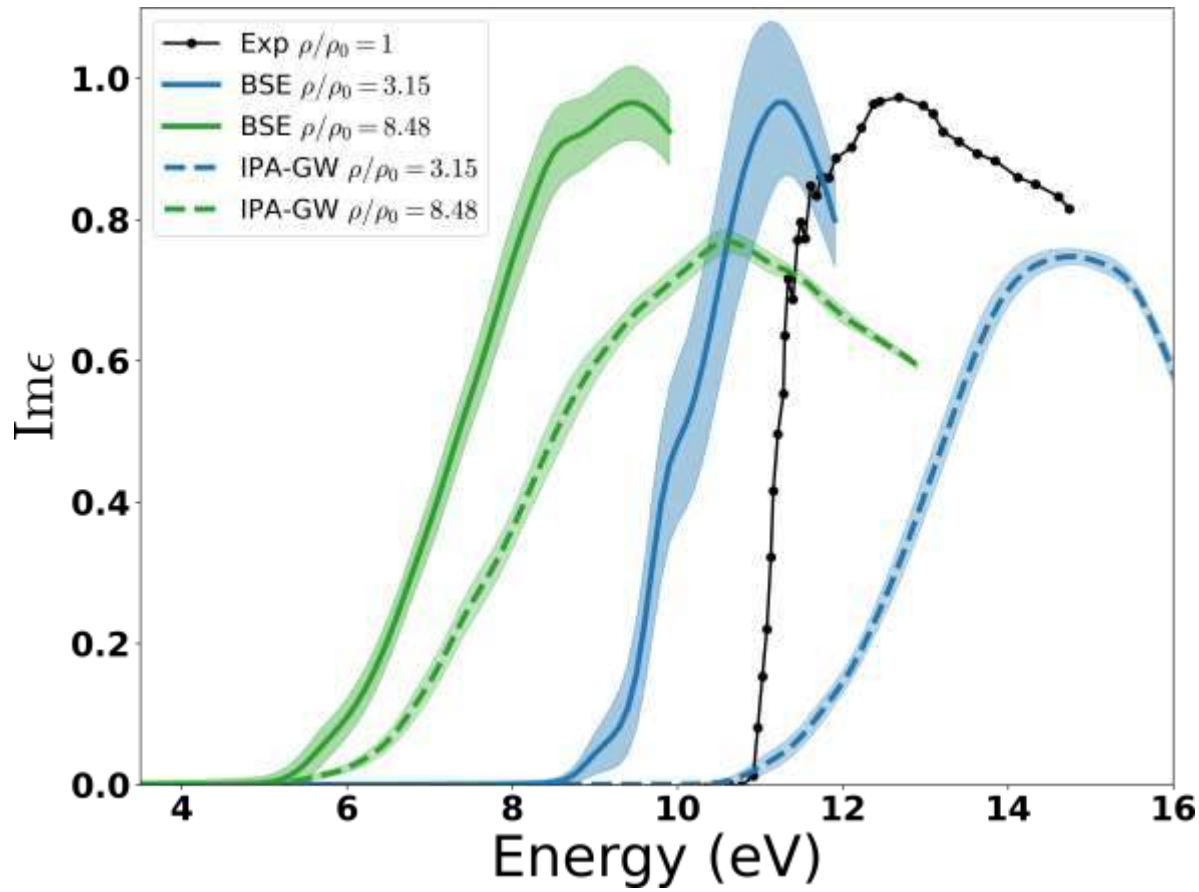

FIG. 3. Absorption spectra from BSE (solid) and IPA-GW (dashed) at $\rho/\rho_0 = 8.48$ (green) and $\rho/\rho_0 = 3.15$ (blue) and experimental spectra at $\rho/\rho_0 = 1$(black) from [30]. We have renormalized the spectra to match the experimental intensity.

Nuclear thermal and quantum effects on the QP gap

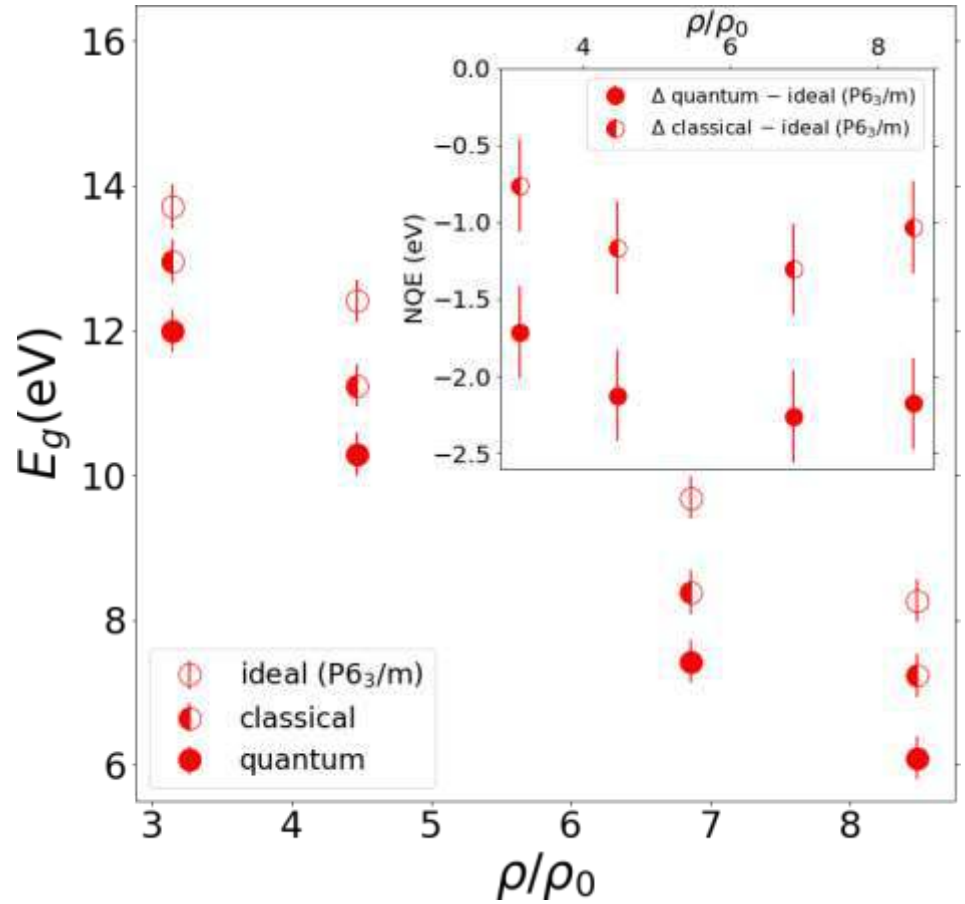

FIG. 3. Quasiparticle (QP) gap of ideal structure with $P\,6_3/m$ structure (open circles), QP gap with classical protons giving only temperature e↵ects and QP gap with quantum protons giving quantum and temperature e↵ects. Inset: The reduction of the quasiparticle gap due to temperature and quantum nuclear e↵ects (filled circled) and only temperature e↵ects (half-filled circles)

Localization of the excitation for neutral gap calculations

For a single nuclear configuration we show the probability of the excited electron having fixed the position of the hole at the center of a molecule and summing over molecular centers.

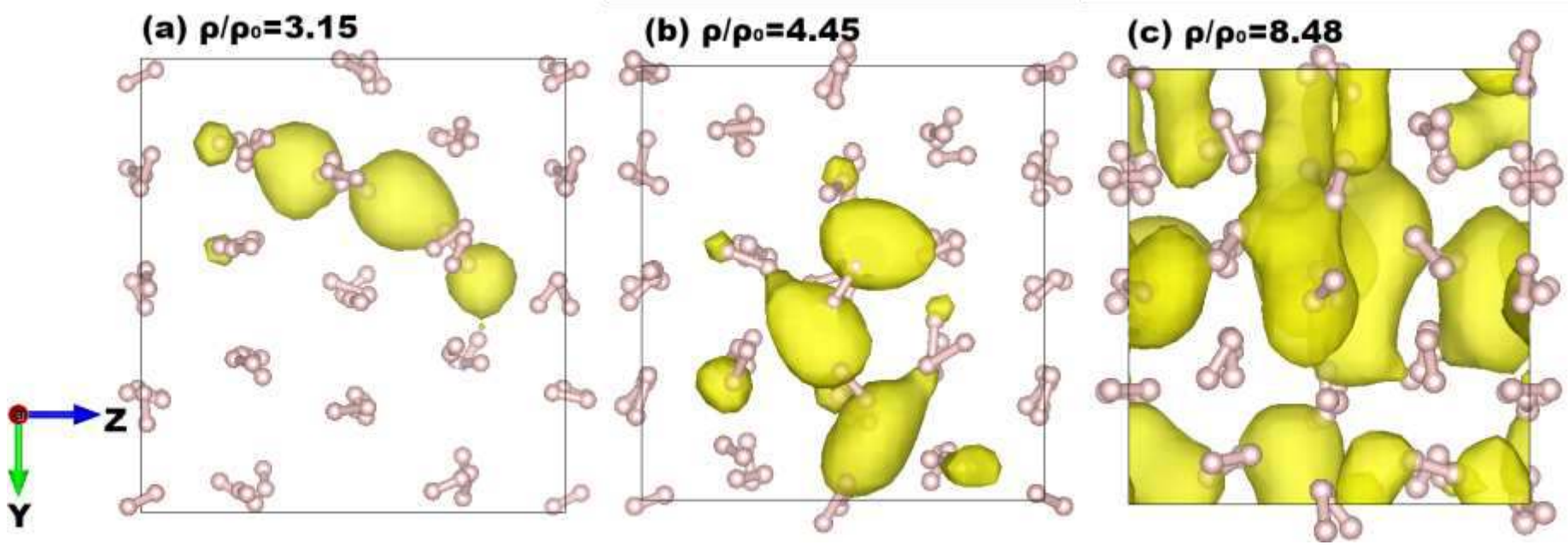

FIG. 14. Spatial distribution of the lowest energy exciton wave function integrated over the hole position $\mathbf{r}_h$: $\int^{R} d\mathbf{r}_h |W_0(\mathbf{r}_h, \mathbf{r}_e)|^2$, see Eq. 10, obtained from BSE calculations for one configuration at different compressions: $\rho/\rho_0 = 3.15$ (left), $\rho/\rho_0 = 4.45$ (middle) and $\rho/\rho_0 = 8.48$ (right). The isosurface level is 10%.

- At the lowest compressions the excitation is almost localized on a single molecule.
- At 10 GPa excitation is delocalized over several molecules but still contained within our supercell.
- At 90 GPa excitation dimension is much larger than our supercell and looks delocalized. Here size effects are of 1/L similar to the QP gap calculation

Conclusions on energy gaps

- QMC and CEIMC allow to investigate hydrogen in various relevant conditions (in particular metallization and molecular dissociation) avoiding the XC approximation of DFT.
- We developed various strategies, all based on QMC, to compute quasi-particle gaps and neutral gaps of insulators.
- We understood finite size effects and related them to the spacial extension of the excitation.
- We computed gaps of ideal structures of Carbon and Silicon finding partial agreement with experiments (but good agreement with previous estimates), but el-phonons and pseudo-potentials effects should be considered.
- We computed the gaps in high-pressure hydrogen finding excellent agreement with experiments, both in phase III and in phase I.
- Our study allows to associate unequivocally the edge of IXS signal in Phase I of hydrogen with the neutral gap, electronic excitation.
- We made predictions for the fluid phase as well (not discussed).

Perspectives

- Multi-determinant methods to investigate excitation localisation and exciton effects: in progress.

THANK YOU FOR YOUR ATTENTION !